Analogous Saturation Mechanisms of the Ion and Electron Temperature Gradient Drift Wave Turbulence

V. Sokolov and A. K. Sen
Plasma Research Laboratory, Columbia University, New York, New York 10027, USA
(Received 25 October 2013; published 25 August 2014)

New experimental results and theoretical arguments indicate that a novel saturation mechanism of the electron temperature gradient modes is related to its coupling to a damped ion acoustic mode. The experimental bicoherence data show multimode coupling between two high frequency radial harmonics of electron temperature gradient in the vicinity of (~2 MHz) and one low frequency ion acoustic (~45 kHz) mode. A unique feedback diagnostic also verifies this coupling. It is pointed out that a near identical mechanism is responsible for ITG mode saturation [V. Sokolov, and A. K. Sen, Phys. Rev. Lett. 92, 165002 (2004)], indicating its plausible generic nature.

DOI: 10.1103/PhysRevLett.113.095001 PACS numbers: 52.35.Kt, 52.35.Mw

Turbulent thermal transport is a fundamental open physics issue in fusion science. The most plausible physics scenario for this anomalous ion and electron transport appears to be based on drift modes: ion temperature gradient (ITG) and electron temperature gradient (ETG) instabilities [1–3].

Ion turbulent transport is fairly well understood. Extensive theoretical and simulation work clearly establish both ion and electron dynamic behaviors, both linear and nonlinear [4–12]. In contrast, experimental validation of theories of electron transport is lacking. The number of experiments about identifications of ETG mode and consequent electron transport is very limited [13–16] due to certain diagnostic problems with the high frequency and short wavelengths of electron turbulence.

We experimentally investigated the novel saturation mechanism of ITG modes in a series of basic experiments in the Columbia Linear Machine (CLM) [17,18]. This mechanism was explained by an unique three-wave coupling of two ITG radial harmonics due to profile variation of ω_T^* [19], and an ion acoustic wave (IA): $\omega_{\mathrm{ITG},l=0} - \omega_{\mathrm{IGT},l=1} \Rightarrow \omega_{\mathrm{IA}}$ [17,18]. We also experimentally studied the complimentary roles of IA damping and zonal flows (ZF) [20] shearing in the saturation of ITG [21]. The stabilizing effect of ZF on the parent ITG modes via flow shear appears to be small [22]. Now we report experimental results and theoretical estimation of nonlinear saturation mechanism of the ETG modes.

The layout of the CLM has been described in Refs. [23,24]. CLM is a steady-state collisionless cylindrical plasma machine with a uniform axial magnetic field (Fig. 1). The typical plasma parameters in the CLM are $n \sim 5 \times 10^9$ cm^{-3}, $B \approx 0.1T$, $T_e \approx 5$–20 eV, and $T_i \approx 5$ eV, the diameter d ~ 6 cm and plasma column length $L \sim 150$ cm, respectively [24]. One needs a strong radial electron temperature gradient to cause an ETG mode. Toward this end, the electrons of the plasma core are effectively heated via parallel acceleration by a positively biased (+20 V) disk mesh (see Fig. 1). The moderate neutral pressure in the transition region guarantees that the accelerated electrons are thermalized to a Maxwellian distribution. Production and identification of the slab ETG mode have been successfully demonstrated in a basic experiment in the CLM [24]. This result has been recently validated by numerical simulation [25]. The first experimental scaling of electron thermal transport coefficient vs amplitude of the ETG mode was also obtained [26].

We now study the nonlinear saturation mechanism of ETG modes. We present the experimental evidence of the coupling of ETG modes and a low frequency mode through experimental bicoherence data. The low frequency mode is identified as the IA mode leading to a three-wave coupling model of two high frequency radial harmonics of ETG modes and one low frequency IA mode. This has been verified by a novel feedback diagnostic.

Figure 2 shows the typical power spectra of plasma potential fluctuations. The mode with frequency $f \sim$ 2 MHz has been identified as an ETG mode with azimuthal

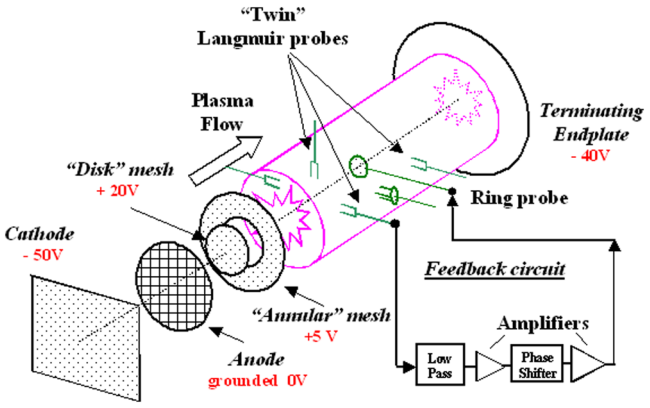

FIG. 1 (color online). Scheme of the CLM and diagnostic setup.

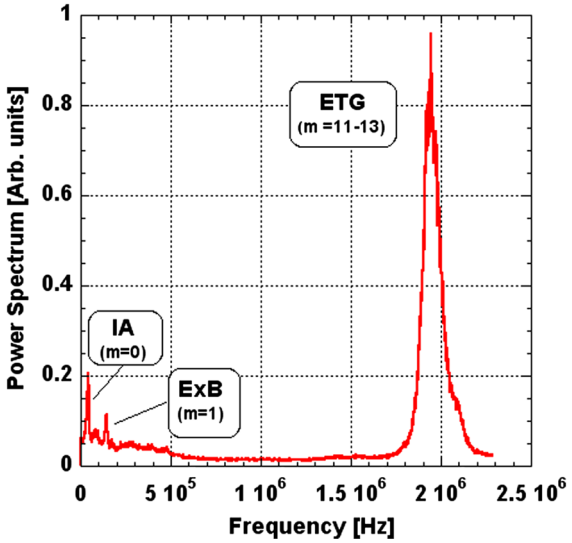

FIG. 2 (color online). Power spectra of potential fluctuation.

wave number $m \sim 11$–13, $k_\perp \rho_e \ll 1$, $k_\perp \rho_i > 1$ and propagating in the electron diamagnetic direction. The characteristic of the drift waves $k_\parallel \ll k_\perp$ is also satisfied by this mode [24]. The mode with frequency $f \sim 140$ kHz has been identified as an $\vec{E} \times \vec{B}$ mode with azimuthal mode number $m = 1$, $k_\parallel = 0$, always present in the CLM [24]. Note also the presence of low frequency fluctuations $f \sim 45$ kHz identified as the IA mode and as described below.

It is noted that in the CLM (as well as in tokamaks), the mode frequency is Doppler shifted by the equilibrium $\vec{E} \times \vec{B}$ rotation of the plasma column with frequency $\omega_E = (m/r)V_{E\times B}$, where m is the azimuthal mode number. In this experiment m was about 11–13. From this it follows that the Doppler shift frequency ω_E also obeys the selection rule of three-wave resonant mode coupling:

$$m_1(\mathbf{k}_1) \pm m_2(\mathbf{k}_2) = m_3(\mathbf{k}_3), \qquad \omega_{E1} \pm \omega_{E2} = \omega_{E3}.$$

It is well known that the presence of three-wave coupling can be determined via bispectrum [27]. The normalized autobispectrum, called the autobicoherency, is defined as

$$b^2(\omega_1, \omega_2) = \frac{|\langle X(\omega_1)X(\omega_2)X^*(\omega_1+\omega_2)\rangle|^2}{\langle|X(\omega_1)X(\omega_2)|^2\rangle\langle|X(\omega_1+\omega_2)|^2\rangle},$$

where $X(\omega_i)$ are Fourier amplitudes.

Figure 3(a) shows a typical bicoherence and the corresponding power spectrum. In the bicoherence figures the X and Y axis are ω_1 and ω_2, respectively, both are in units of kHz/2π. We note that the dense patches of contours on the diagonal in the ω_1-ω_2 plane represent self-coupling of modes, while the off-diagonal patches indicate cross coupling of modes. The bicoherence corresponding to cross coupling between the ETG mode ω_1 and the low frequency $\omega_2 \sim 2\pi \times 45$ kHz mode is seen Fig. 3(a) as a horizontal patch and dense horizontal contours in Fig. 3(b);

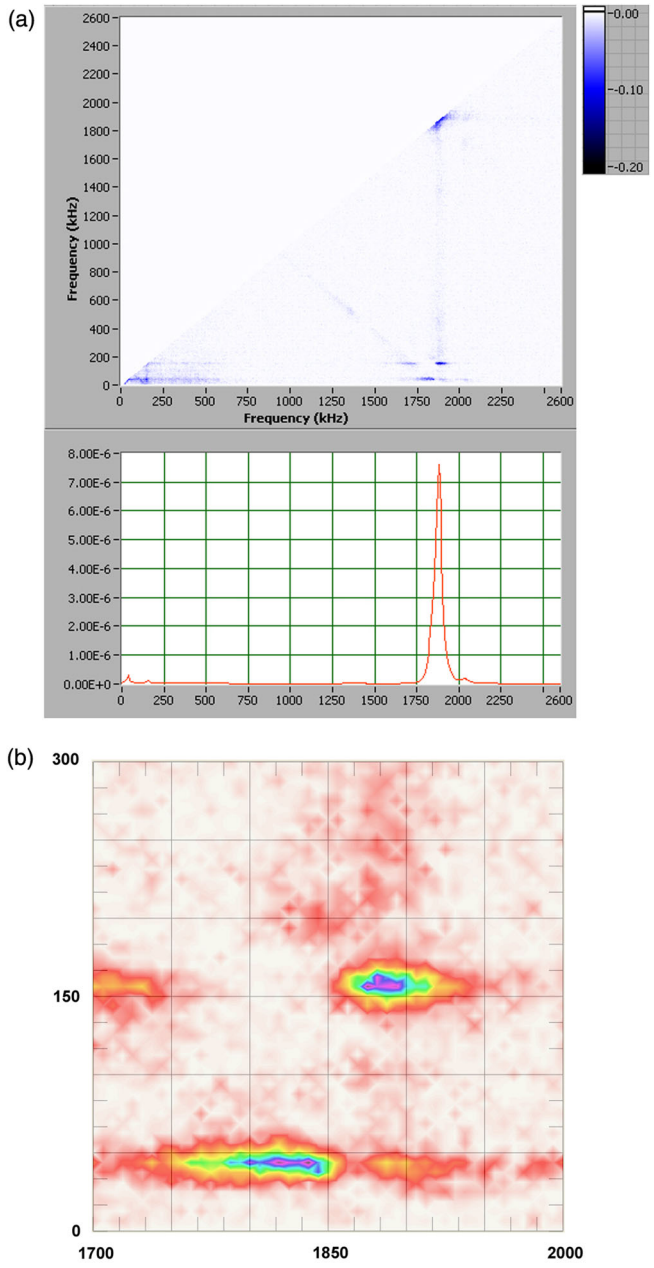

FIG. 3 (color online). The bicoherence of ETG mode coupling, frequency units are in kHz. (a) Bicoherence and corresponding power spectrum. (b) A close-up of the bicoherence.

the value of bicoherence is $b^2 \sim 0.1$. This may indicate mode coupling between one low frequency mode $\omega_2 \sim 2\pi \times 45$ kHz, which is visible in the low frequency end of the power spectrum (see Fig. 2) and two higher frequency radial harmonics, $\omega_1 = \omega_{12\_1}$ $(m = 12,\ l = 1) \sim 2\pi \times 1.85$ MHz, $\omega_3 = \omega_{12\_0} (m = 12, l = 0) \sim 2\pi \times 1.9$ MHz of ETG modes. Therefore, this can be considered as multimode interaction leading to saturation via the damped ion acoustic mode. Here, m, l refer to the azimuthal and radial harmonic mode numbers, respectively, as described below.

Parenthetically, we tried to directly drive a pure IA mode via appropriately biased ring probe (see Fig. 1) in the absence of drift wave turbulence. We found this was not possible, presumably due to its strong damping [28].

It is noted that two weak patches with $\omega_2 \sim 2\pi \times$ 140 kHz in Fig. 3 Correspond to three-wave coupling of two ETG modes and the $E \times B$ mode. The right weak patch is $\omega_{\mathrm{ETG},m=12} + \omega_{E\times B,m=1} \Rightarrow \omega_{\mathrm{ETG},m=13}$ and the left patch is $\omega_{\mathrm{ETG},m=11} + \omega_{E\times B,m=1} \Rightarrow \omega_{\mathrm{ETG},m=12}$.

The solution of the fluid eigenmode equation for the slab ITG mode with nonuniform temperature gradient profiles [18,19] yields its radial harmonics. Figure 4 shows the radial profiles of the electron temperature and the inverse temperature scale length $[L_{T_e}(r)]^{-1} = -d(\ln T_e)/dr$. Using the isomorphism of the electron and ion response we can obtain the same fluid eigenmode equation [18,19,29] for the ETG mode with nonuniform $\omega^*_{T_e}(r)$ and small $(\mathrm{k}_\theta \rho_e)^2$ as

$$\frac{d^2\tilde{\phi}}{dx^2} - \left(k_\theta^2 - \frac{\left(\frac{k_\parallel v_{T_e}}{\omega}\right)^2 \frac{\omega_{T_e}}{\omega} + \tau}{\rho_e^2 \left(\left(\frac{k_\parallel v_{T_e}}{\omega}\right)^2 \frac{\omega_{T_e}}{\omega} - 1 \right)} \right) \tilde{\phi} = 0, \quad (1)$$

where $\omega_{T_e} = \omega_{T_e}(r) = \omega^*_{T_e}(r) = k_\theta \rho_e \kappa_{T_e}(r) \rho_e \Omega_{ce}$, ω_{T_e} is the electron temperature gradient diamagnetic drift frequency, $\kappa_{T_e}(r) = -d(\ln T_e)/dr$ is the inverse temperature scale length, and $\tau = T_{e/}/T_i$. Equation (1) is a Weber type equation and its solution can be described in terms of Hermite polynomials [19] as

$$\left(\frac{k_\parallel v_{T_e}}{\omega_{T_e}}\right)^2 + \tau \left(\frac{\omega}{\omega_{T_e}}\right)^3 = \left(\frac{k_\parallel v_{T_e}}{\omega_{T_e}}\right) \left(\frac{\omega}{\omega_{T_e}}\right)^{3/2} \sqrt{(\tau+1)\frac{\omega^\parallel_{T_e} \rho_e^2}{2\omega_{T_e}}}(2l+1), \quad (2)$$

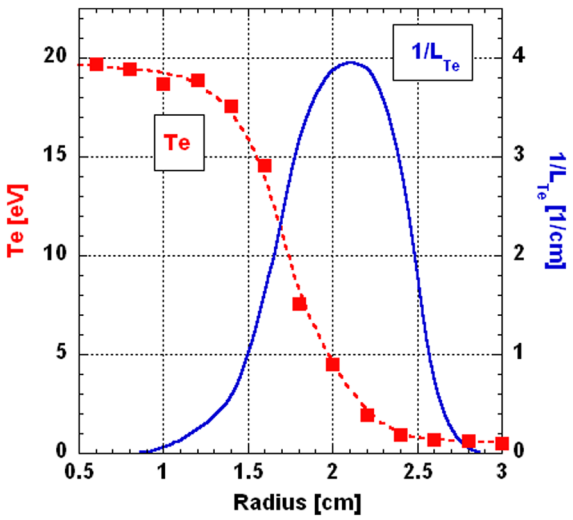

FIG. 4 (color online). Radial profiles of electron temperature and inverse scale length $1/L_{T_e} = -d(\ln T_e)/dr$.

where the double prime indicates the second radial derivative and l is the radial mode number.

We find a perturbative solution of the above as $\omega = \omega_0 + \delta\omega$, where ω_0 is the local solution and $\delta\omega$ is the nonlocal correction [19,29]. Then Eq. (2) yields

$$\frac{\delta\omega}{\omega_{T_e}} = \frac{-\sqrt{3}+i}{6\tau^{5/6}} \left(\frac{k_\parallel v_{T_e}}{\omega_{T_e}}\right)^{2/3} \sqrt{(\tau+1)\frac{\omega^\parallel_{T_e}\rho_e^2}{2\omega_{T_e}}}(2l+1). \quad (3)$$

For two radial harmonics ω_{12_0} ($m = 12$, $l = 0$) and ω_{12_1} ($m = 12, l = 1$), with CLM parameters we obtain $\Delta\omega = \omega_{12\_0} - \omega_{12\_1} \sim 2\pi^*(30)$ kHz, which is close to the low frequency third mode of the triad discussed above. This validates the three-wave coupling interpretation of bicoherency data shown above.

We now discuss in detail the identification of the low frequency mode of the triad discussed above. Its azimuthal mode number m_3 is determined from the set of azimuthal phase shift measured via cross correlation of two high frequency Langmuir probes [24], displaced azimuthally 90° and 180° (see Fig. 1) apart to yield $m_3 = 0$. The parallel wavelength is determined from the axial phase shift measured via cross correlation of two other Langmuir probes, displaced axially by 28.5 cm (see Fig. 1). The resulting phase shift for typical plasma parameters shown in Fig. 5 indicates that it is a linear function of frequency in the 30–60 kHz range. The reciprocal of the slope of this line (see Fig. 5) yields a phase velocity of 3.5×10^6 cm/ sec, which is in a very good agreement with ion acoustic wave speed $\mathrm{C_s} \sim 4 \times 10^6$ cm/ sec calculated for the CLM parameters. Therefore, the low frequency mode in the triad

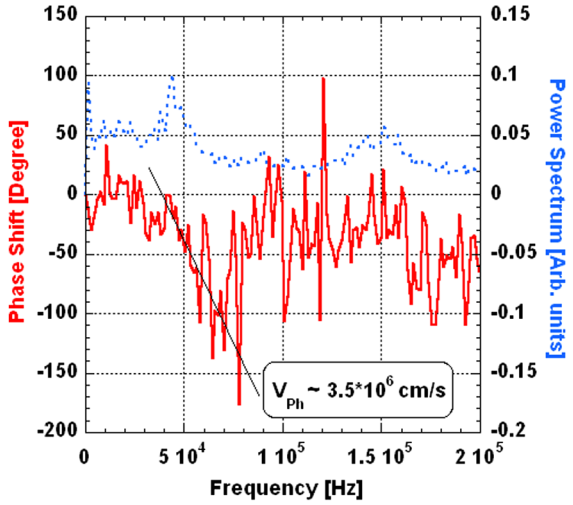

FIG. 5 (color online). Measurement of the parallel phase velocity of the low frequency mode. The dashed line shows the power spectrum, the solid line is the phase shift between two axial probes.

of three-wave coupling is a plane ion acoustic (IA) mode with $m_3 = 0$ and $\omega_3/2\pi = 45$ kHz.

Bicoherence alone is not a proof of a saturation mechanism, it only indicates mode coupling—which is one of the canonical nonlinear phenomena in plasma dynamics [30]. However, if and only if at least one of these modes is damped (ion acoustic mode in our case), mode coupling will lead to saturation.

We now present another additional experimental evidence of coupling between ETG modes and the low frequency ion acoustic mode. This evidence is based on probing the coupling via feedback diagnostic, which is unique in CLM (see Fig. 1). We use one of the high frequency Langmuir probes [24] as a sensor and an specially designed ring Langmuir probe as an actuator of the feedback circuit (see Fig. 1). We used the ring shape of the probe to enhance the efficiency of the actuator and for excitation of the plane wave with $m = 0$. The ring probe has a radius of 1.2 cm and wire diameter of 0.2 mm and is placed coaxial with the plasma column. The radius of the ring probe is smaller than the radius where the maximum of the ETG mode amplitude is located at 1.8 cm [24]. Its influence in exciting an ETG mode is found to be not significant. The frequency band of the feedback loop was limited by a low pass electronic filter at <100 kHz. We used the ring probe as electrically floating and our feedback signal has an ac component only (amplitude $\leq 0.1\ k^* T_e/e$, phase shift ~180°). The phase and amplitude feedback signal are adjusted by a phase shifter and amplifiers (see feedback circuit in Fig. 1). The results of feedback experiments with different levels of feedback gain shown in Fig. 6 indicate that the amplitude of ETG modes (high frequency ~2 MHz) changed with the changing of the low frequency (~45 kHz) mode under feedback control, whereas other plasma parameters remained the same. Therefore, it is a clear demonstration of nonlinear mode coupling between the high frequency modes (ETG) and the low frequency mode (IA).

It is noted that in the absence of feedback three-wave coupling is a closed system. For a closed system, if one mode amplitude goes up another mode must go down. Feedback opens up the system and allows energy to flow in and out. In this case, when one mode goes up in amplitude, another mode may also go up.

A theory of three-wave coupling of two ETG harmonics and IA mode [29] estimated the saturation level of the ETG mode about $\varphi_{\mathrm{rms}} \sim 10\%$ for CLM parameters, which is within the range of the experimental values and not inconsistent with gyrokinetic simulation results for tokamaks. This mode coupling scenario is novel in view of the fact that most mode-coupling theories are restricted to coupling only in azimuthal (poloidal) wave numbers of the same mode, unlike here.

In conclusion, the experimental bicoherence data show coupling between two high frequency (~2 MHz) and one low frequency (~45 kHz) modes. Measurements of azimuthal wave number ($m = 0$) and parallel wave vector ($k_\parallel \approx \omega/C_s$) clear identify that the low frequency mode is a plane IA wave. The theoretical estimation from the nonlocal dispersion relation for ETG radial harmonics gives the difference between the radial harmonics to be about 30 kHz, not that far from the frequency of the IA mode, indicating multimode interaction. A novel feedback diagnostic independently verified this nonlinear coupling between the low frequency mode (IA) and the high frequency mode (ETG). It is surmised that this mechanism may be valid for the saturation of all drift waves.

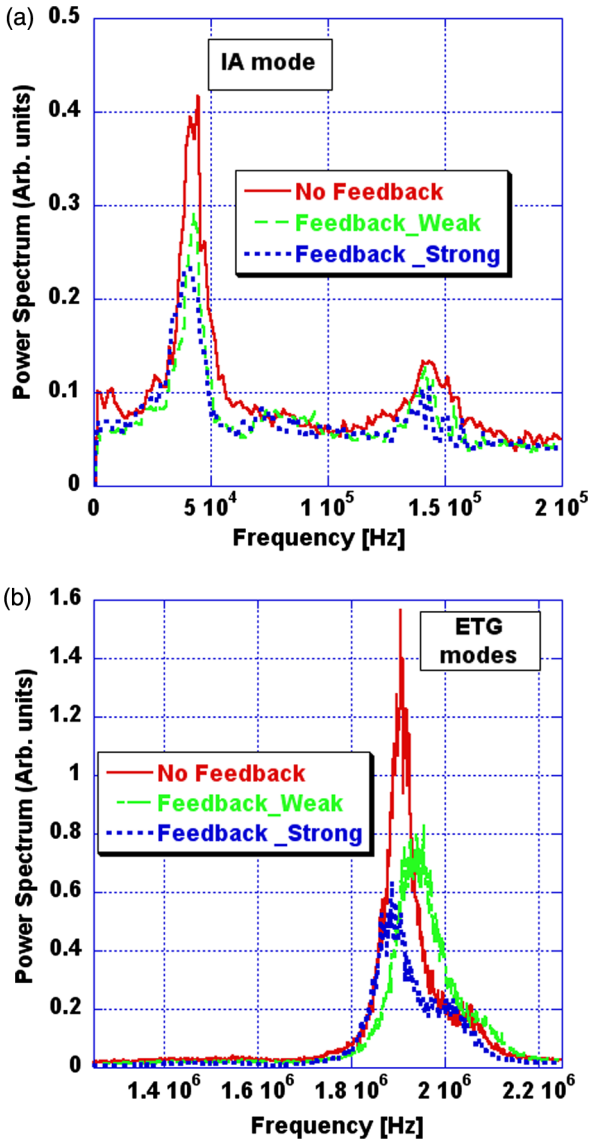

FIG. 6 (color online). The power spectra of potential fluctuations vs different levels of feedback gain. The "Strong" level corresponds to $\sim 0.1 k^* T_e/e$ and the "Weak" level is about $0.03 k^* T_e/e$. (a) Low frequency part (IA mode). (b) High frequency part (ETG mode).

One of the most interesting implications of this study is the near ubiquitous role of damping in collisionless plasmas provided by ion acoustic damping. It may be the collisionless analog to viscous damping in classical fluid mechanics.

This research was supported by U.S. Department of Energy Grant No. DE-FG02-98ER-54464.

[1] B. Coppi and G. Rewoldt, in *Advances in Plasma Physics*, edited by A. Simon and W. B. Thompson (Wiley, New York, 1976), Vol. 6, p. 421.
[2] W. Horton, Rev. Mod. Phys. **71**, 735 (1999).
[3] F. Jenko and W. Dorland, Phys. Rev. Lett. **89**, 225001 (2002).
[4] W. Dorland, F. Jenko, M. Kotschenreuther, and B. N. Rogers, Phys. Rev. Lett. **85**, 5579 (2000).
[5] Y. C. Lee, J. Q. Dong, P. N. Guzdar, and C. S. Liu, Phys. Fluids **30**, 1331 (1987).
[6] W. Horton, B. G. Hong, and W. M. Tang, Phys. Fluids **31**, 2971 (1988).
[7] Z. Lin, L. Chen, and F. Zonca, Phys. Plasmas **12**, 056125 (2005).
[8] W. Horton, H. V. Wong, P. J. Morrison, A. Wurm, J. H. Kim, J. C. Perez, J. Pratt, G. T. Hoang, B. P. LeBlanc, and R. Ball, Nucl. Fusion **45**, 976 (2005).
[9] W. M. Nevins *et al.*, Phys. Plasmas **13**, 122306 (2006).
[10] R. E. Waltz, J. Candy, and M. Fahey, Phys. Plasmas **14**, 056116 (2007).
[11] A. M. Dimits *et al.*, Nucl. Fusion **47**817 (2007).
[12] U. Zakir, Q. Haque, and A. Qamar, Phys. Plasmas **20**, 052106 (2013).
[13] L. Schmitz, A. E. White, T. A. Carter, W. A. Peebles, T. L. Rhodes, W. Solomon, and K. H. Burrell, Phys. Rev. Lett. **100**, 035002 (2008).
[14] E. Mazzucato *et al.*, Phys. Rev. Lett. **101**, 075001 (2008).
[15] E. Z. Gusakov, A. D. Gurchenko, A. B. Altukhov, A. Yu. Stepanov, L. A. Esipov, M. Yu. Kantor, and D. V. Kouprienko Plasma Phys. Controlled Fusion **48**, A371 (2006).
[16] C. Moon, T. Kaneko, and R. Hatakeyama, Phys. Rev. Lett. **111**, 115001 (2013).
[17] V. Sokolov and A. K. Sen, Phys. Rev. Lett. **92**, 165002 (2004).
[18] V. Sokolov and A. K. Sen, Nucl. Fusion **45**, 439 (2005).
[19] S. E. Parker and A. K. Sen, Phys. Plasmas **9**3440 (2002).
[20] P. H. Diamond, S.-I. Itoh, K. Itoh, and T. S. Hahm, Plasma Phys. Controlled Fusion **47**, R35 (2005).
[21] V. Sokolov, X. Wei, A. K. Sen, and K. Avinash, Plasma Phys. Controlled Fusion **48**, S111 (2006).
[22] V. Sokolov and A. K. Sen, Phys. Rev. Lett. **104**, 025002 (2010).
[23] R. Scarmozzino, A. K. Sen, and G. A. Navratil, Phys. Fluids **31**, 1773 (1988).
[24] X. Wei, V. Sokolov, and A. K. Sen, Phys. Plasmas **17**, 042108 (2010).
[25] X. R. Fu, W. Horton, Y. Xiao, Z. Lin, A. K. Sen, and V. Sokolov, Phys. Plasmas **19**, 032303 (2012).
[26] V. Sokolov and A. K. Sen, Phys. Rev. Lett. **107**, 155001 (2011).
[27] Y. C. Kim and E. J. Powers, IEEE Trans. Plasma Sci. **7**, 120 (1979).
[28] R. J. Goldston and P. H. Rutherford, *Introduction to Plasma Physics* (Taylor & Francis Group, LLC, New York, 1995).
[29] E. K. Tokluoglu, V. Sokolov, and A. K. Sen, Phys. Plasmas **19**, 102306 (2012).
[30] R. Z. Sagdeev and A. A. Galeev, *Nonlinear Plasma Theory* (W.A. Benjamin, Inc. New York, 1969).